

Indexing a Discrete Global Grid

A. Vince

Department of Mathematics

University of Florida

Gainesville, FL 32611-8105

USA

`vince@math.ufl.edu`

Abstract

In an increasingly interconnected world, the development of computer friendly systems for the display and analysis of global data is an important issue. This paper concerns a method for computer representation and manipulation of global data based on multi-resolution subdivisions of regular polyhedra. In particular, the problem of efficiently indexing the cells of such a discrete global grid is addressed.

1 Digital Earth

The subject of this report, the representation and analysis of global data, has a history that dates back several millenia. Maps, possibly the earliest depiction of geographical information, are easily understood and appreciated regardless of language or culture. The oldest known maps are preserved on Babylonian clay tablets from about 2300 B.C. That the Earth is spherical was known by Greek philosophers by the time of Aristotle (about 350 B.C.). Ptolemy's map (about 85-165 A.D.) depicted the Old World from about 60N to 30S latitudes. The first whole world maps began to appear in the early 16th century, following voyages by Columbus and others to the New World. In 1569 Mercator published a map of the world intended as an aid to navigation, using a projection method now known by Mercator's name. Buckminster Fuller invented the geodesic dome in the late 1940's. Geographic information systems (GIS) emerged in the 1970-80s. The emphasis over the past few decades has been on the computer display and analysis of georeferenced information and remotely sensed data about the Earth, collected by organizations and institutions. As more global datasets are acquired and as the world becomes more interconnected, this endeavor becomes increasingly important.

This paper concerns such a computer representation of global data, called a *discrete global grid*, that is based on cellular subdivisions of regular polyhedra. An array of data consists of one data element for each grid cell. The user has the flexibility to define the meaning of grid cell values according to the application at hand. Traditional digital image processing in the plane is carried out on a rectangular grid. For some applications, however, hexagonal grids are advantageous. Hexagonal grids have a higher packing density, approximate circular regions, and each cell has equal distance from its six immediate neighbors. The most commonly used grids on the sphere are those based on latitude-longitude coordinates. On the sphere, however, an (almost) hexagonal grid is an even more natural choice than in the plane. The hexagons have almost the same shape and size as compared with a lat/long grid.

There is a substantial recent literature on the subject of spherical grids based on tessellations of regular polyhedra, including [1, 3, 8, 13]. One commonly mentioned is an aperture 3, multi-resolution tessellation of the sphere into mainly hexagons. *Multi-resolution* means that there is not just a single tessellation, but a hierarchical sequence of progressively finer tessellations. Going further in the sequence zooms in on smaller areas. *Aperture 3* refers to the approximate ratio between the areas of hexagons at successive tessellations in the sequence. In fact, this small ratio is one of the features that makes an aperture 3 tessellation appealing. Such a tessellation of the sphere will be referred to as an *aperture 3 hexagonal discrete global grid* (A3H). A mathematical construction is given in Section 2 of this paper. Figure 1 shows a few levels of resolution of such an A3H.

Of the numerous research challenges in the field, this paper concentrates on the problem of efficiently addressing or indexing the cells of A3H. While Section 2 describes the geometry and basic data structure of A3H, the rest of the paper provides two methods of indexing its cells, which we call barycentric indexing and radix indexing. The first method, based on an investigation of the barycenters of the cells in A3H, was developed in [18]. The second is based on a generalization of the concept of positional number systems (radix systems) for the integers [17]. The particular radix system discussed here for A3H was developed in conjunction with Canadian based company the PYXIS innovation [12]. Each of the two methods has advantages in providing efficient algorithms for the relevant applications. Indexing based on quad tree data structures is appropriate for certain discrete global grids not discussed in this paper [2, 5, 7, 11, 15]. Proofs of theorems appearing in this paper have been referenced but not included.

2 The geometry of A3H

A3H is obtained by tessellating a regular polyhedron, then projecting the tessellated polyhedron onto the surface of the sphere. For this paper the relevant regular polyhedra are the octahedron and the icosahedron. Before giving the construction, the following basic geometric operations are introduced.

The *barycenter* $\beta(X)$ of a set $X = \{\mathbf{x}_1, \mathbf{x}_2, \dots, \mathbf{x}_n\}$ of points in \mathbb{R}^3 is given by

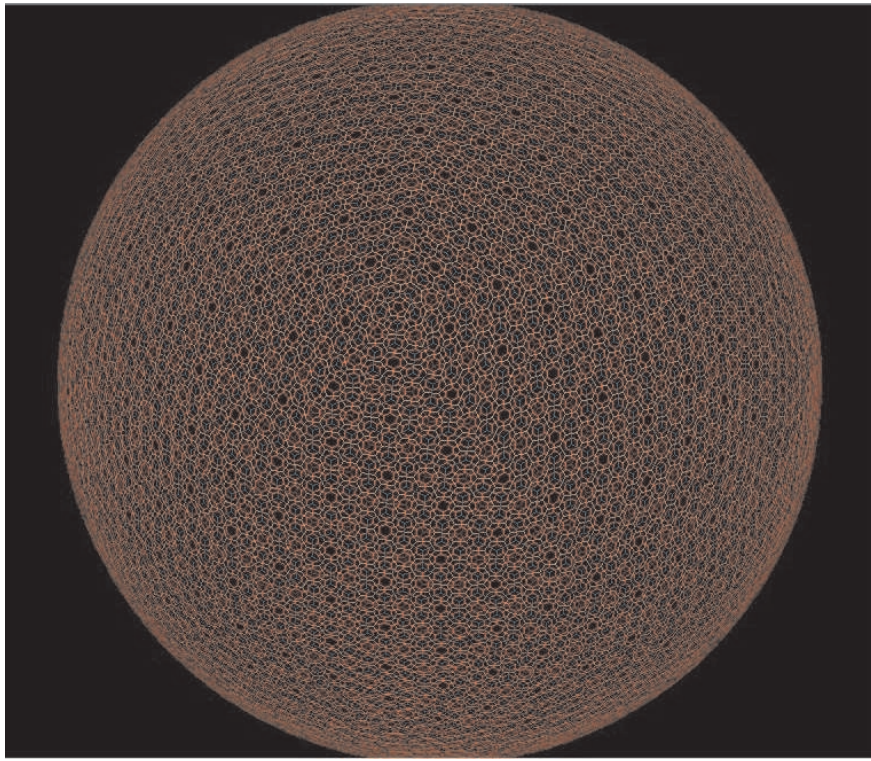


Figure 1: A3H.

$$\beta(X) = \frac{1}{n} \sum_{i=1}^n \mathbf{x}_i.$$

By a *tessellation* T of a polyhedron or of the sphere, we mean a collection of closed, non-overlapping cells that cover the surface. On a polyhedron the edges are straight lines and, on the sphere, arcs of great circles. For a tessellation T , the notation $V(T)$ and $E(T)$ denote the set of vertices and edges, respectively. For a tessellation T let

$$\beta(T) = \{\beta(t) \mid t \in T\}$$

denote the set of barycenters of its cells. (Here t is considered as the set of its three vertices.) Two basic operations on tessellations are the dual and centroid subdivision. They are defined as follows and illustrated in Figure 2.

1. *The dual.* For a tessellation T with vertex set V , the dual tessellation $D(T)$ has vertex set $\beta(T)$. Two vertices of $D(T)$ are joined by an edge if and only if the corresponding cells of T share an edge.
2. *Centroid subdivision.* The centroid subdivision $C(H)$ of tessellation H has vertex set $V(H) \cup \beta(H)$. The edge set of $C(H)$ is the union of $E(H)$ and the set of edges formed by joining $\beta(h)$ to each vertex of h for all $h \in H$.

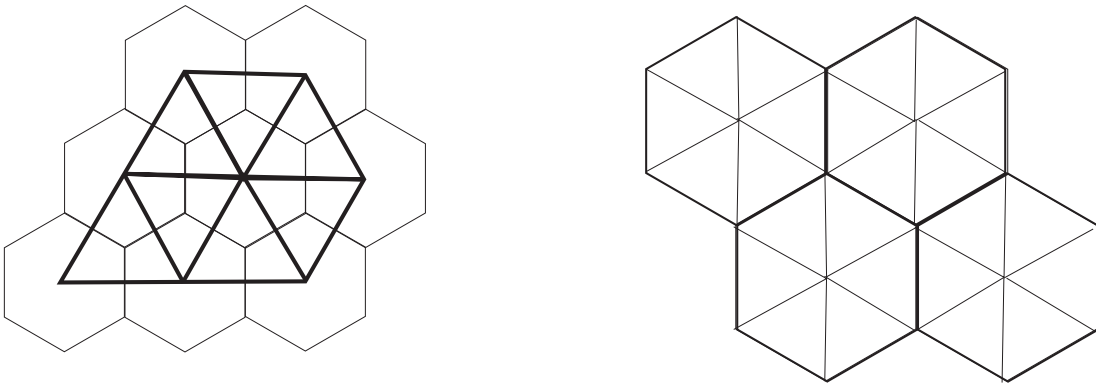


Figure 2: Basic operations on a tessellation.

Construction

Let P be either the regular octahedron or icosahedron. Define a sequence (T_n, H_n) of dual pairs of tessellations of P as follows. First, T_0 is the polyhedron itself centered at the origin of \mathbb{R}^3 . The sequence is then defined recursively in terms of the dual and centroid subdivision:

$$H_n = D(T_n)$$

$$T_{n+1} = C(H_n).$$

The sequence $H_n, n \geq 0$, of tessellations is the one called the A3H. We leave open until the next section whether A3H is based on the octahedron or icosahedron, i.e., whether T_0 is the octahedron or icosahedron. The number n is called the *resolution* of A3H. The dual tessellations T_n and H_n are shown, in part, in Figure 3. In fact, Figure 3 shows a patch of two successive subdivisions T_n, T_{n+1} and H_n, H_{n+1} . Note that $V_n := V(T_n)$ is the set of cell centers of the the tessellation H_n .

Properties

The following properties of A3H are either obvious or easily proved by induction.

1. The tessellation T_n is a triangulation for each n , i.e., the faces are triangles. Moreover, the triangulation T_n contains exactly $c \cdot 3^n$ triangles where $c = 8$ or 20 depending on whether T_0 is an octahedron or icosahedron.
2. The n^{th} resolution H_n of A3H contains exactly $\frac{c}{2}(3^n - 1)$ hexagons and either 6 squares or 12 pentagons, depending on whether T_0 is an octahedron or icosahedron.
3. The sets of barycenters of cells of the A3H are nested: $V_0 \subset V_1 \subset V_2 \subset \dots$.
4. The ratio of the area of a hexagon in H_n to the area of a hexagon in H_{n+1} is 3.

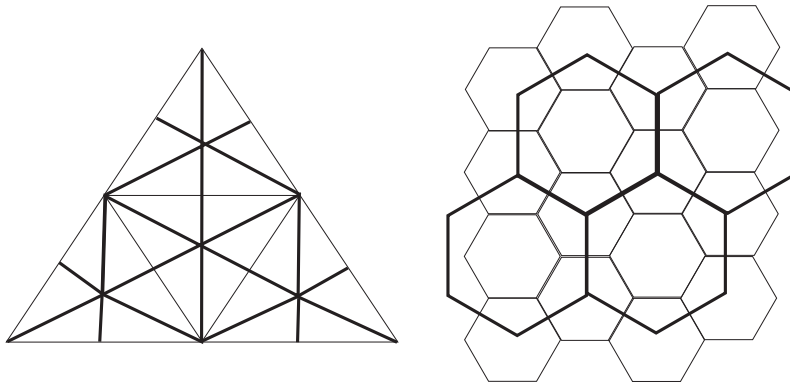


Figure 3: Two successive subdivisions.

5. Each hexagonal (pentagonal) cell x of H_n intersects exactly 7 cells (6 cells) of H_{n+1} , a *centroid cell*, with the same barycenter as x , and 6 *vertex cells* (5 vertex cells) whose centers are the vertices of x . See Figure 3.
6. Each cell $x \in H_n$ intersects either 1 or 3 cells of H_{n-1} , one cell in the case that x is a centroid cell, three cells in the case that x is a vertex cell.

Projection onto the Sphere

There are various methods for projecting $A3H$ from the tessellated polyhedron onto the surface of the 2-dimensional sphere, for example by central projection from the origin. No projection method can be both equal area (areas related by a constant scaling factor) and conformal (angles preserved). One of the most common equal area projections, due to Snyder, is well suited to the icosahedron and is called the *icosahedral Snyder equal area projection* (ISEA3H). The projection formulas can be found in [14].

3 Indexing A3H

Recall that the n^{th} resolution of A3H is denoted H_n . The set of barycenters of the cells in H_n is denoted V_n and, when no confusion arises, we will identify a cell with its barycenter. Indexing is a means to reference or address the cells in H_n (points in V_n). So an *index function* is an injection

$$I : V_n \rightarrow W_n,$$

where W_n is referred to as the *index set*. A good index function is one that allows for efficient implementation of algorithms for the relevant applications. This requires the efficient handling of relevant data structures and fast algebraic operations on indices corresponding to local vector operations on the cell centers. In Sections 4 and 5 two methods are introduced for indexing A3H.

4 Barycentric Indexing

Barycentric indexing of the cells of A3H is based on the tessellations of the regular octahedron as described in Section 2. Thus T_0 is the octahedron centered at the origin of \mathbb{R}^3 , and H_0 , the 0^{th} resolution of A3H, is the cube. The first resolution H_1 is the truncated octahedron. As will be explained soon, the index set W_n consists of all strings of $n + 3$ digits, each digit taken from the set $\{-1, 0, 1\}$ of “trits”. Thus the index set W_n has size $27 \cdot 3^n$ while H_n has $4 \cdot 3^n + 2$ cells.

To define the index function, first place the vertices of the octahedron T_0 at the six points $(\pm 1, 0, 0)$, $(0, \pm 1, 0)$, $(0, 0, \pm 1)$ in \mathbb{R}^3 . Theorem 1 gives the Cartesian coordinates of the set V_n of cell centers of A3H on the surface of the octahedron (prior to projection onto the sphere). The proofs of Theorems 1-3 appear in [17]. All congruences in this section are modulo 3.

Theorem 1 *The set V_n of barycenters of cells of the octahedral A3H at resolution n is given by*

$$V_n = \begin{cases} \left\{ \frac{1}{3^{\frac{n}{2}}} (a, b, c) : a, b, c \in \mathbb{Z}, |a| + |b| + |c| = 3^{\frac{n}{2}} \right\} & \text{if } n \text{ is even} \\ \left\{ \frac{1}{3^{\frac{n+1}{2}}} (a, b, c) : a, b, c \in \mathbb{Z}, |a| + |b| + |c| = 3^{\frac{n+1}{2}}, a \equiv b \equiv c \right\} & \text{if } n \text{ is odd.} \end{cases}$$

Define the *A3-coordinates* of a point in V_n , or the corresponding cell in H_n , as the ordered triple (a, b, c) of integers as given in Theorem 1. In other words the A3-coordinates of the cell with center $(1/3^{\frac{n}{2}}) (a, b, c)$, n even, or $(1/3^{\frac{n+1}{2}}) (a, b, c)$, n odd, is simply (a, b, c) . Hence the A3-coordinates of a cell of H_n is an ordered triple (a, b, c) of integers such that

$$|a| + |b| + |c| = 3^{\frac{n}{2}} \quad \text{if } n \text{ is even}$$

$$\begin{aligned} |a| + |b| + |c| &= 3^{\frac{n+1}{2}} \\ a &\equiv b \equiv c \pmod{3} \end{aligned} \quad \text{if } n \text{ is odd.}$$

Given the A3-coordinates of a cell x , the location of x in terms of the Cartesian coordinates of its center is immediately known via Theorem 1. Each cell $x \in H_n$ is adjacent to either 5 or 6 cells called *neighbors* of x . The *centroid and vertex children* of x are the centroid and vertex cells, respectively, of x , as defined by Properties 5 and 6 in Section 2. Call the cells at resolution $n - 1$ that overlap x the *parents* of x . Theorems 2 and 3 give simple rules, in terms of A3-coordinates, for the following basic procedures that are essential for global grid applications. Given the A3-coordinates of an arbitrary cell x at any resolution,

- determine the neighbors, children, and parents of x ; and
- perform local algebraic operations in the vicinity of the cell.

Theorem 2 *A3 addressing satisfies the following properties.*

1. *The neighbors of a cell in H_n with A3-coordinates (a_1, a_2, a_3) have A3-coordinates (b_1, b_2, b_3) , where, for $i = 1, 2, 3$,*

$$|a_i - b_i| \leq \begin{cases} 1 & \text{if } n \text{ is even} \\ 2 & \text{if } n \text{ is odd.} \end{cases}$$

2. *The centroid child in H_{n+1} of $(a, b, c) \in H_n$ is*

$$\begin{cases} 3(a, b, c) & \text{if } n \text{ is even} \\ (a, b, c) & \text{if } n \text{ is odd.} \end{cases}$$

3. *Cell $(a, b, c) \in H_n$ is a centroid child if and only if*

$$\begin{cases} a \equiv b \equiv c & \text{if } n \text{ is even} \\ a \equiv b \equiv c \equiv 0 & \text{if } n \text{ is odd.} \end{cases}$$

4. *The vertex children of (a, b, c) are, in either the even or odd case, the neighbors of the centroid child as given by item (1).*

5. *The parent in H_{n-1} of a centroid child $(a, b, c) \in H_n$ is*

$$\begin{cases} (a, b, c) & \text{if } n \text{ is even} \\ \frac{1}{3}(a, b, c) & \text{if } n \text{ is odd.} \end{cases}$$

6. *Let $x = (a, b, c) \in H_n$ be a vertex child.*

For n even, the cell x has exactly three neighbors (d, e, f) with the property that $d \equiv e \equiv f$. These three are the A3-coordinates of the parents of (a, b, c) in H_{n-1} .

For n odd, the cell x has exactly three neighbors (d, e, f) with the property that $d \equiv e \equiv f \equiv 0$. For these three the triples $\frac{1}{3}(d, e, f)$ are the A3-coordinates of the parents of (a, b, c) .

Using the A3-coordinates, a local vector arithmetic can be efficiently implemented as follows. By “local” we mean centered at any cell of H_n and restricted to a single face of the octahedron. By “vector arithmetic” we mean usual vector addition and multiplication by scalars for vectors contained on a single face of the octahedron.

The *octant* of a triple (a, b, c) of integers is the ordered triple of signs (+ or $-$) of the three entries. The octant of $(5, -2, 2)$, for example, is $(+, -, +)$. Two points of V_n lie on the same face of the octahedron if and only if their A3-coordinates are in the same octant. Let \mathbf{x}_0 be the A3-coordinates of a fixed cell $x_0 \in H_n$. Let \mathbf{x}_1 and \mathbf{x}_2 be the A3-coordinates of two other cells $x_1 \in H_n$ and $x_2 \in H_n$ in the same octant as \mathbf{x}_0 . Let \mathbf{v}_1 denote the vector pointing from the center of x_0 to the center of x_1 ; similarly \mathbf{v}_2 the vector pointing from the center of x_0 to x_2 .

- Theorem 3** 1. With notation as given above, the vector sum $\mathbf{v}_1 + \mathbf{v}_2$ points from \mathbf{x}_0 to $\mathbf{x}_1 + \mathbf{x}_2 - \mathbf{x}_0$, where the sum of the \mathbf{x}_i in the above formula is the usual addition in \mathbb{R}^3 . The formula is valid as long as $\mathbf{x}_1 + \mathbf{x}_2 - \mathbf{x}_0$ lies in the same octant as \mathbf{x}_0 .
2. For an integer k , the scalar product $k \mathbf{v}_1$ points from \mathbf{x}_0 to $k \mathbf{x}_1 + (1 - k) \mathbf{x}_0$.

We have shown that each A3H cell can be represented as an ordered triple of integers called the A3-coordinates. An indexing scheme for A3H is now introduced for referencing the cells at any level of resolution n using a string of $n + 3$ “trits.” The *balanced ternary* is a base 3 positional number system using the digit set $D = \{-1, 0, 1\}$, with D often referred to as the set of *trits*. The integer 8, for example, has the balanced ternary representation $8 = (1)(0)(-1)$. Relevant to our application are the following properties of the balanced ternary. Further information can be found in Knuth’s “The Art of Computer Programming” [9].

1. Every integer, positive or negative, has a unique representation in the balanced ternary. Moreover, every integer between $-3^n/2$ and $3^n/2$ has a unique representation of the form

$$\sum_{k=0}^{n-1} d_k 3^k,$$

where $d_k \in D$.

2. The negative of an integer in balanced ternary is obtained by merely changing the sign of each digit.
3. Two integers in balanced ternary are congruent modulo 3 if and only if they have the same last digit. In particular, an integer is divisible by 3 if and only if the last digit in its balanced ternary representation is 0.

Given A3-coordinates (a, b, c) , encode this triple as a string S of $n + 3$ trits as follows. The cases n even and odd are considered separately.

Even $n = 2k$. The first $k + 1$ trits in S represent the integer a .

The second $k + 1$ trits represent the integer b .

The third integer c is given by the formula $c = \pm(3^k - |a| - |b|)$, where the ± 1 is the last trit in S .

Odd $n = 2k - 1$. The first $k + 1$ trits in S represent the integer a .

The second $k + 1$ trits represent the integer b .

The third integer c is given by the formula $c = \pm(3^k - |a| - |b|)$, where the \pm is chosen to make $a \equiv b \equiv c \pmod{3}$.

The index function $I : V_n \rightarrow W_n$ for A3H is now defined as follows. For a point $x \in V_n$, let (a, b, c) be its A3-coordinates, and let S be the balanced ternary string encoding of (a, b, c) as explained above. Then define $I(x) = S$. It should now be

apparent, from Theorems 1, 2, and 3 and the stated properties of the balanced ternary, that the essential operations on the cells of the octahedral A3H can be performed using elementary base 3 arithmetic applied to the indices.

5 Radix Indexing

The indexing function for A3H introduced in this section is based on tessellations of the regular icosahedron. Thus T_0 is the regular icosahedron; H_0 is the dodecahedron; and the first resolution H_1 is the truncated icosahedron. The indexing is first defined on planar “tiles.” Thirty two such tiles are then assembled to form the icosahedral A3H.

This indexing scheme is based on a 2-dimensional generalization of positional number systems for the integers. It is a fundamental result in number theory that if b is an integer greater than 1, then every positive integer has a unique representation of the form

$$\sum_{i=0}^N b^i \cdot d_i,$$

where the digits d_i belong to a set $D = \{0, 1, 2, \dots, b-1\}$. It was remarked in the previous section that every integer, positive or negative, has a unique representation of the above form if $b = 3$ and $D = \{-1, 0, 1\}$. This is the balanced ternary system. The set of integers is a 1-dimensional lattice. Analogous positional number systems exist for higher dimensional lattices. A 2-dimensional *lattice* is the set of all integer linear combinations of two linearly independent vectors in \mathbb{R}^2 . The *hexagonal lattice* is the lattice generated by the vectors $(1, 0), (\frac{1}{2}, \frac{\sqrt{3}}{2})$. Call a triple (L, B, D) a 2-dimensional *radix system* if L is a 2-dimensional lattice, B is linear map (2×2 matrix) such that $B(L) \subset L$, and D is a finite subset of L that includes the origin. The set D is called the *digit set* and B the *base*. A natural, but difficult, question is for which radix systems does there exist a unique representation of each lattice point $x \in L$ in the form

$$x = \sum_{i=0}^N B^i(d_i), \tag{1}$$

where $d_i \in D$. See [16] for partial answers and references. As is standard for the base 10 radix system $(\mathbb{Z}, (10), \{0, 1, 2, 3, 4, 5, 6, 7, 8, 9\})$, for any radix system we will use the abbreviated notation

$$x = d_N d_{N-1} \cdots d_1 d_0$$

instead of the form (1).

For the purposes of this paper, L is the hexagonal lattice. The base is 3, more precisely B is the linear transformation given by multiplication by 3. The hexagonal lattice L is the set of centers of the hexagonal grid and, if no confusion arises, we will identify each lattice point in L with the corresponding hexagon of which it is the center. For the set of digits, initially take

$$D' = \{0, 1, \omega, \omega^2, \omega^3, \omega^4, \omega^5, \omega + \omega^2, \omega^4 + \omega^5\},$$

these 9 lattice points shown as shaded hexagons in Figure 4, where in complex number notation $\omega = \frac{1}{2} + \frac{1}{2}\sqrt{3}i$. Although the proof is omitted, this radix system (L, B, D') has the property that every point in L has a unique representation in the form given in equation (1) above.

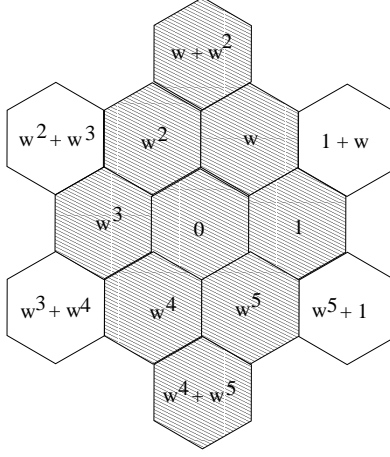


Figure 4: Digit set.

Next expand the digit set D' with 9 elements to the digit set

$$D = \{0, \omega^k, \omega^{k-1} + \omega^k : 1 \leq k \leq 6\}$$

with 13 elements as shown in Figure 4. To simplify notation, for $1 \leq k \leq 6$, make the following replacements:

$$\begin{aligned} \omega^k &\leftarrow 0k \\ \omega^k + \omega^{k+1} &\leftarrow k0. \end{aligned} \tag{2}$$

Hence in the radix system (L, B, D) , each lattice point $x \in L$ can be expressed as $x = (e_{2N+1} e_{2N}) \cdots (e_3 e_2) (e_1 e_0)$ or simply

$$x = e_{2N+1} e_{2N} \cdots e_3 e_2 e_1 e_0, \tag{3}$$

where each $e_i \in \{0, 1, 2, 3, 4, 5, 6\}$. In the radix system (L, B, D) the representation of lattice points in the form of equation (1), equivalently (3), is no longer unique. For example the lattice point $1 + \omega$ (see Figure 4) can be expressed as either 0140 or 60 because $0140 = (01)(40) = 3\omega + (\omega^4 + \omega^5) = 1 + \omega = \omega^6 + \omega^7 = 60$. We have used the identities $\omega^6 = 1$ and $1 + \omega^2 + \omega^4 = 0$, which can also be used to prove the following theorem.

Theorem 4 *In the hexagonal radix system (L, B, D) every element of L can be written uniquely in the form (3) with the restriction that there exist no two consecutive non-zero digits, i.e., between any two non-zero digits there is at least one zero.*

In analogy to decimals, next introduce the notation $.e_1 e_2 \cdots e_{2N-1} e_{2N}$, where $e_i \in \{0, 1, 2, 3, 4, 5, 6\}$ with no two consecutive non-zero digits. Before the replacement (2) this is $.d_1 d_2 \cdots d_N$, where $d_i \in D$, which stands for

$$x = \sum_{i=1}^N 3^{-i} \cdot d_i, \quad d_i \in D.$$

Define \mathbf{P}_n to be the set all points in the plane of the form $.e_1 e_2 \cdots e_n$ where $e_i \in \{0, 1, 2, 3, 4, 5, 6\}$ with no two consecutive non-zero digits. If n is odd, the implicit $(n+1)^{st}$ digit is 0. For ease of notation, the decimal point will be dropped. For example, 105 represents the point in the plane:

$$(10) \frac{1}{3} + (50) \frac{1}{9} = (\omega + \omega^2) \frac{1}{3} + (\omega^5 + 1) \frac{1}{9} = \frac{1}{9} (5\omega - 1).$$

The set \mathbf{P}_n is a subset of points of an hexagonal lattice, the larger the n , the finer the lattice (points closer together). The integer n will be referred to as the *resolution* of \mathbf{P}_n . Figure 5 shows two resolutions \mathbf{P}_1 and \mathbf{P}_3 . (For clarity, the set \mathbf{P}_2 is omitted from the figure, but each hexagon of \mathbf{P}_2 has area in the ratios 1/3 and 3 to the hexagons in \mathbf{P}_1 and \mathbf{P}_3 , respectively, and each hexagon of \mathbf{P}_2 is rotated by 30° relative to those in \mathbf{P}_1 and \mathbf{P}_3 .) For a given hexagon (or corresponding lattice point), the string $e_1 e_2 \cdots e_n$ will be referred to as its *index*. If W_n is the set of all strings of length n with elements from the set $\{0, 1, 2, 3, 4, 5, 6\}$, no two consecutive non-zero, then define

$$I : \mathbf{P}_n \rightarrow W_n$$

by $I(x) = e_1 e_2 \cdots e_n$ for $x \in \mathbf{P}_n$. The indices are also shown in Figure 5. The next result lists properties of the sets \mathbf{P}_n , $n \geq 0$. (Note that \mathbf{P}_0 consists just of the origin.)

Theorem 5 *The set \mathbf{P}_n , $n \geq 0$, satisfy the following properties.*

1. *The \mathbf{P}_n are nested: $\mathbf{P}_0 \subset \mathbf{P}_1 \subset \mathbf{P}_2 \subset \cdots$.*
2. *The ratio of the area of a \mathbf{P}_n hexagon to the area of a \mathbf{P}_{n+1} hexagon is 3.*
3. *The hexagons in \mathbf{P}_n , n even, are oriented a 30° rotation to the hexagons in \mathbf{P}_n , n odd.*
4. *The number of hexagons in \mathbf{P}_n is $\frac{1}{5}(3^{n+2} - (-2)^{n+2})$.*
5. *\mathbf{P}_n has 6-fold rotational symmetry about the origin.*

Tree Data Structure

The data structure underlying the sets \mathbf{P}_n , $n \geq 0$, has the form of a tree \mathbf{T} . The set of nodes of \mathbf{T} is $\cup \{P_n : n \geq 0\}$. The nodes at depth n are the cells at resolution n . Each node x at depth n has 7 children, one at level $n+1$ and six at depth $n+2$. The child x_0 at depth $n+1$ is the centroid cell (as defined by Property 5 in Section

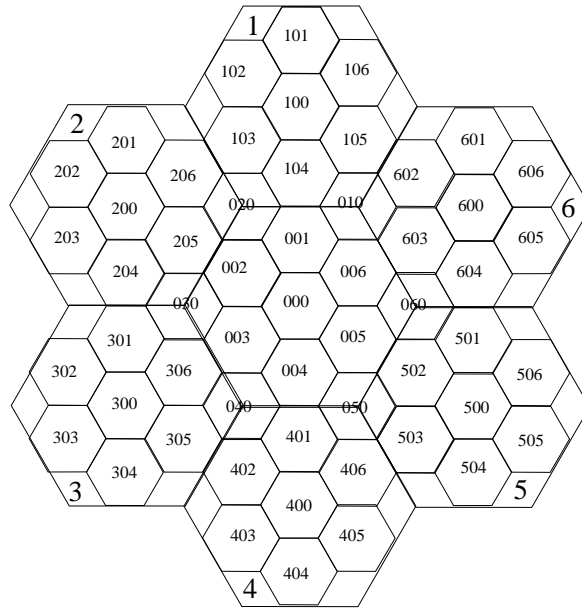


Figure 5: \mathbf{P}_1 and \mathbf{P}_3 .

2) of x while the six children at depth $n + 2$ are the vertex cells of x_0 . Note that the children and parents of a cell as defined in Section 4 do not correspond exactly to the children and parent of a cell in \mathbf{T} . The basic idea here is that each cell x at resolution n generates

- one *centroid child* x_0 at resolution $n + 1$ with the same center as x , and
- five or six *vertex children* at resolution $n + 2$ centered at the vertices of x_0 .

It can be shown that the indexing is closely related to the data structure. If $\alpha \in W_n$ is the index of a hexagon of \mathbf{P}_n at resolution n , then

- $\alpha 0 \in W_{n+1}$ is the index of its centroid child, and
- $\alpha 0 k \in W_{n+2}$, $1 \leq k \leq 6$, are the indices of its 6 vertex children.

Face tiles and Vertex Tiles

The sets \mathbf{P}_n will be referred to as a *face tiles*. The construction is now altered slightly to obtain a vertex tile. For each $1 \leq k \leq 6$ construct a set $\mathbf{P}_{n,k}$ as follows. The set \mathbf{P}_n can be partitioned into 6 subsets, each one approximately a 60° wedge of \mathbf{P}_n . More precisely, for $1 \leq k \leq 6$, let $\mathbf{P}_n^{(k)}$ be the set of all $x \in \mathbf{P}_n$ such that the first non-zero digit in the index $I(x)$ is k . Let $P'_{n,k}$ denote the set of hexagons obtained from \mathbf{P}_n by removing those in $\mathbf{P}_n^{(k)}$

$$P'_{n,k} = \mathbf{P}_n \setminus \mathbf{P}_n^{(k)}.$$

Given an index α , let α^+ denote the result of adding 1 (modulo 6) to every non-zero digit in α . Now construct $\mathbf{P}_{n,k}$ as follows. Remove the edge in $P'_{n,k}$ that is contained only on the hexagon centered at the origin. The hexagon at the origin now becomes a pentagon. Identify, in pairs, the other edges in $P'_{n,k}$ that are contained on exactly one hexagon of $P'_{n,k}$ as follows. Identify each such edge common to hexagons with indices α and β in \mathbf{P}_n with the edge common to hexagons α^+ and β^+ . Whereas each \mathbf{P}_n possesses 6-fold rotational symmetry about the origin, each $\mathbf{P}_{n,k}$ possesses 5-fold symmetry. Geometrically the six sets $\mathbf{P}_{n,k}$, $1 \leq k \leq 6$, are identical, but their indexing is not. With the indexing ignored, denote each $\mathbf{P}_{n,k}$ simply by \mathbf{P}_n^* . While \mathbf{P}_n is planar, \mathbf{P}_n^* is not. The tile \mathbf{P}_n^* is called a *vertex tile*.

Indexing the Icosahedral A3H

We are now in a position to define the radix indexing on the icosahedral A3H. It is based on the following theorem, which is illustrated in Figure 6 depicting the 20 faces of the icosahedron flattened onto the plane.

Theorem 6 *For each $n \geq 1$, the $(n+1)^{st}$ resolution H_{n+1} of A3H is the non-overlapping union of 20 copies of face tile \mathbf{P}_{n-1} , each such tile centered at the barycenter of a triangular face of the icosahedron, and 12 copies of vertex tile \mathbf{P}_n^* , each such tile centered at a vertex of the icosahedron.*

In Figure 6, H_2 is shown as a non-overlapping union of 20 copies of \mathbf{P}_0 (a single hexagon at the center of each triangle of the icosahedron) and 12 copies of \mathbf{P}_1^* (6 cells centered at each vertex of the icosahedron). For clarity, the identifications of the edges of \mathbf{P}_1 to form \mathbf{P}_1^* has not been made in the figure. Also the indices are omitted.

The indexing at resolution $n + 1$ on A3H is inherited from the indexing on copies of tiles \mathbf{P}_{n-1} and \mathbf{P}_n^* . Label the vertices of the icosahedron U_k, U'_k , $1 \leq k \leq 6$, where U_k and U'_k are antipodal to each other. Then at vertices U_k and U'_k of H_{n+1} provide the indexing of patch $\mathbf{P}_{n,k}$. Label the faces of the icosahedron F_k , $1 \leq k \leq 20$. At face F_k of H_{n+1} provide the indexing of patch \mathbf{P}_{n-1} . There still remains some ambiguity because of the possible rotations of the patches about their centers (6-fold symmetry of face tiles and 5-fold symmetry of vertex tiles). In practice the vertex tiles are labeled A-T and the face tiles 1-12, their relative positions given by a table.

6 Conclusion

This paper concerned the display and processing of global data on a discrete global grid, in particular, on the aperture 3 hexagonal discrete global grid A3H. After a brief geometric description, the focus was on the problem of indexing the cells of A3H. Two indexing schemes were introduced, barycentric indexing on the octahedral A3H and radix indexing on the icosahedral A3H, both leading to efficient processing.

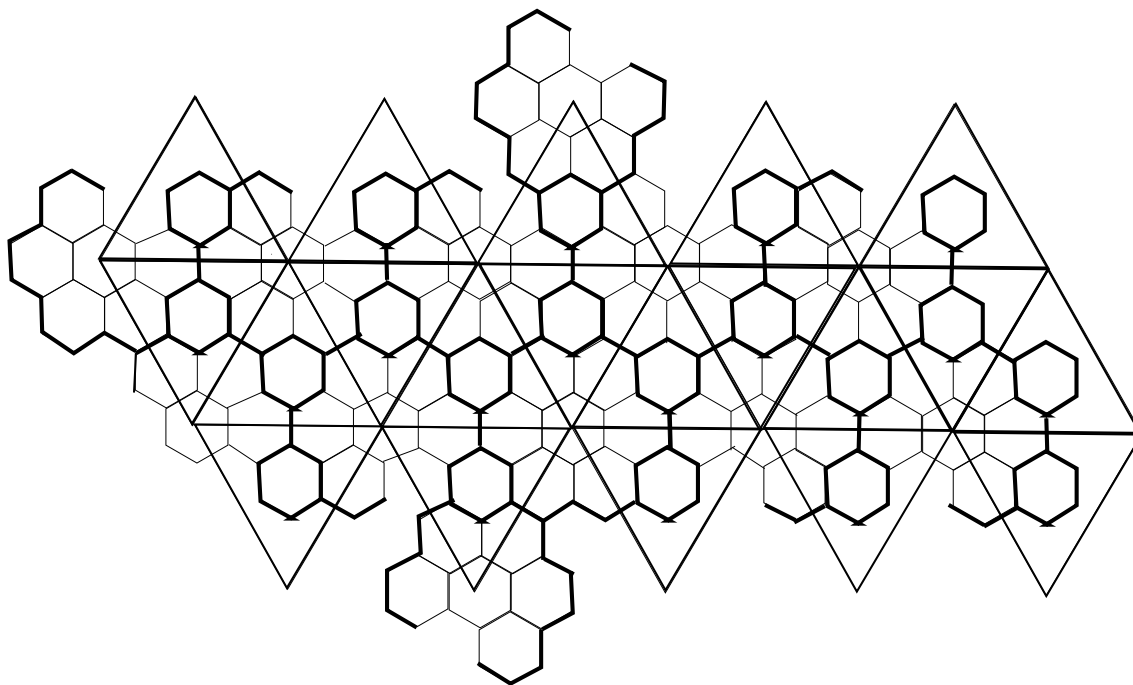


Figure 6: Unfolded Icosahedron

References

- [1] N. Ahuja, On approaches to polygonal decomposition for hierarchical image representation. *Computer Vision, Graphics, and Image Processing* **24** (1983), 200–214.
- [2] P. Barrett, Application of the linear quadtree to astronomical databases. *Proceedings of Astronomical Data Analysis Software and Systems IV, ASP Conference Series, Vol. 77, Astronomical Society of the Pacific* (1995), 472–478.
- [3] J.R. Baumgardner and P.O. Frederickson, Icosahedral discretization of the two-sphere, *SIAM Journal on Numerical Analysis* **22** (1985), 1107–1115.
- [4] S.B.M. Bell and F.C. Holroyd, Lattice rings: coordinates for self-similar hierarchies and their relevance to geographic information systems, *International Journal of Geographical Information Systems* **10** (1996), 147–177.
- [5] J. Chen, X. Zhao, and Z. Li, An algorithm for the generation of Voronoi diagrams on the sphere based on QTM, *Photogrammetric Engineering and Remote Sensing* **69** (2003), 79–90.
- [6] G. Dutton, A hierarchical coordinate system for geoprocessing and cartography, *Lecture Notes in Earth Science* 78, Springer-Verlag, Berlin, 1998.

- [7] G. Fekete and L. Treinish, Sphere quadrees: a new data structure to support the visualization of spherically distributed data. *Proceedings of the SPIE, Extracting Meaning from Complex Data: Processing, Display, Interaction, Vol. 1259, International Society for Optical Engineering* (1990), 242–253.
- [8] M.F. Goodchild and Y. Shiren, 1992. A hierarchical spatial data structure for global geographic information systems, *Computer Vision, Graphics, and Image Processing* **54** (1992), 31–44.
- [9] D.E. Knuth, *The Art of Computer Programming*, Upper Saddle River, N.J., Addison-Wesley, 2005.
- [10] M. Lee M and H. Samet, Traversing the triangle elements of an icosahedral spherical representation in constant time, *Proceedings of the 8th International Symposium on Spatial Data Handling, International Geographical Union, Burnaby, BC.* (1998), 22–33.
- [11] E.J. Otoo EJ and H. Zhu, Indexing on spherical surfaces using semi-quadcodes, *Proceedings of Third International Symposium on Advances in Spatial Databases, Lecture Notes in Computer Science 692*, Springer-Verlag, Singapore (1993), 510–529.
- [12] P.R. Peterson, Close-Packed, Uniformly Adjacent, Multiresolutional, Overlapping Spatial Data Ordering, *Canadian Patent Application 2,436,312*, August 2003.
- [13] K. Sahr, D. White, and A.J. Kimmerling, Geodesic discrete global grid systems. *Cartography and Geographic Information Science*, **30** (2003), 121–134.
- [14] J. P. Snyder, An equal-area map projection for polyhedral globes, *Cartographica* **29** (1992), 10–21.
- [15] A.S. Szalay, J.Gray, G. Fekete, P.Z. Kunszt, P. Kukol, and A. Thakar, Indexing the sphere with the hierarchical triangular mesh, *Technical report, Microsoft Research*, 2005.
- [16] Radix representation and rep-tiling, *Congressus Numerantium* **98** (1993), 199–212.
- [17] A. Vince, Replicating tessellations, *SIAM J. Discrete Math.* **6** (1993), 501–521.
- [18] A. Vince, Indexing the Aperture 3 Hexagonal Discrete Global Grid, preprint.